How Dendrons Stiffen Polymer Chains: A SANS Study

Stephan Förster*

Max-Planck-Institut für Kolloid- und Grenzflächenforschung, Am Mühlenberg, D-14424 Potsdam-Golm, Germany

Ingo Neubert and A. Dieter Schlüter

Institut für Organische Chemie, Freie Universität Berlin, Takustrasse 3, D-14195 Berlin, Germany

Peter Lindner

Institut Laue-Langevin, Ave. des Martyrs, BP 156, F-38042 Grenoble Cedex 9, France

Received November 18, 1998; Revised Manuscript Received April 2, 1999

ABSTRACT: The conformation of various polystyrene chains with first (G-1), second (G-2), and third generation (G-3) Fréchet-type dendrons at the repeat unit has been investigated with small-angle neutron scattering. The increased density of the attached dendrons leads to a systematically greater cross-sectional chain diameter *D*. Bulky, high generation dendrons force the polymer backbone out of its all-trans conformation. The measured statistical Kuhn segment length initially increases in proportion to the chain diameter and then to a greater degree due to steric overcrowding and the concomitantly higher bending rigidity. The introduction of charges further leads to chain expansion and the development of interchain correlations. High molecular weight (G-2) chains develop fully excluded-volume chain properties with a Flory exponent of $\nu = 0.57$ and a critical exponent $\gamma = 0.86$ which is related to the enhancement of chain configurations with widely separated chain ends.

Introduction

Since their discovery some 20 years ago, dendritic macromolecules have stimulated an almost explosive research effort, and many synthetic, analytical, and application-related issues have been addressed.[1] Recently, polymers with bulky dendritic side chains have received considerable interest.[2] The dendrons cause a change in chain conformation that is characterized by the persistence length and excluded volume. Dendrons provide a unique possibility for stiffening polymeric chains in a well-defined way.

In a recent study we showed that polystyrene chains carrying third generation (G3) dendrons exhibit a rodlike conformation in solution.[3] This raises the question of how and to what extent dendrons of a given generation can stiffen polymer chains. In the present study we investigate the conformation of polystyrene chains carrying different first (G-1), second (G2), and third generation (G-3) dendrons using small-angle neutron scattering. By a quantitative analysis of the scattering curves, insight is provided into how dendrons increase the chain diameter and chain stiffness until a rodlike conformation is reached.

Experimental Part

The dendronized polymers (Figure 1) were prepared from the corresponding vinyl monomers by radical polymerization. Details of the synthesis have been reported elsewhere.[4,5] Molecular weights and molecular weight distributions of the dendronized polymers determined by GPC in THF[6] calibrated with narrow molecular weight polystyrenes are given in Table 1 together with other characteristic molecular parameters.

Small-Angle Neutron Scattering. The measurements were performed at the 20.0, 5.0, and 1.1 m detector position at the D11 small-angle instrument at ILL, Grenoble. The neutron wavelength was $\lambda = 0.6$ nm with $\Delta\lambda/\lambda = 8\%$ (from fwhm). Details of the instrumentation and data reduction can be found elsewhere.[7] Polymer concentrations were 5 g/L in order to minimize intermolecular correlations but still have

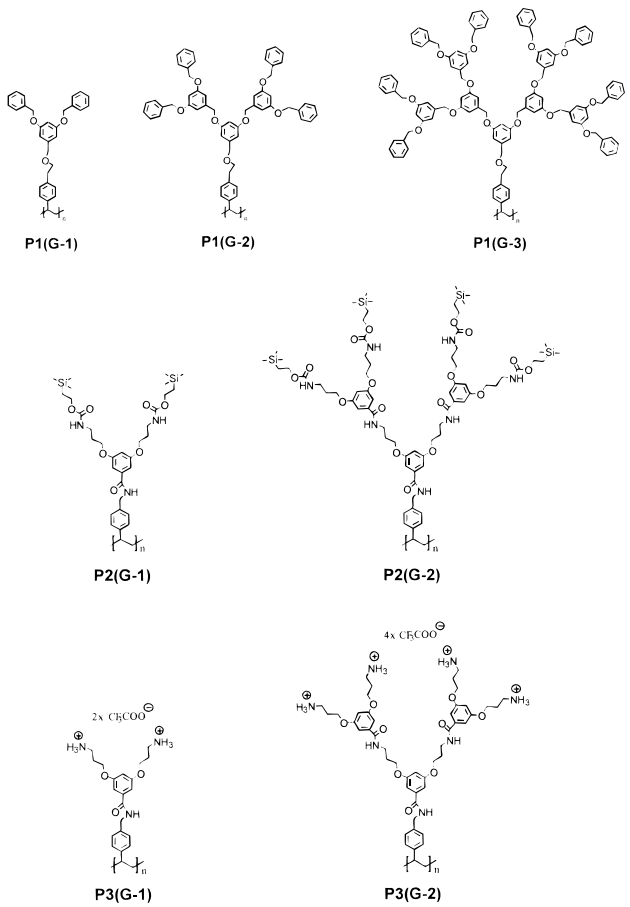

Figure 1. Molecular structure of the dendronized polymers P1(G-1), P1(G-2), P1(G-3), P2(G-1), P2(G-2), P3(G-1), and P3-(G-2).

10.1021/ma9817929 CCC: $18.00
Published on Web 05/22/1999

Table 1. Monomer Molecular Weight M_0, Monomer Molecular Weight per Unit Length M_0/l_0, Specific Density of the Polymers in the Respective Solvent ρ, Neutron Contrast Factor k, Weight-Average Molecular Weight As Determined by GPC M_w^{GPC}, and Polydispersity M_w/M_n of the Polymers in the Present Study[a]

sample	M_0 (g/mol)	M_0/l_0 (g/(mol Å))	ρ (g/cm^3)	k (cm^2 mol/g^2)	M_w^{GPC} (g/mol)	M_w/M_n
PS/CS_2	112.2	44.9			50 000	1.15
P1(G-1)/C_6D_6	450.6	180.2	1.157	0.001 66	79 700	1.6
P1(G-2)/C_6D_6	706.9	282.8	1.250	0.001 23	621 000	1.5
P1(G-3)/C_6D_6	1724.1	689.6	1.241	0.001 21	141 000	3.2
P2(G-1)/CD_3OD	672.0	268.8	1.223	0.002 38	277 000	2.3
P2(G-2)/CD_3OD	1461.0	584.4	1.322	0.001 92	83 500	1.6
P3(G-1)/D_2O	611.5	244.6				2.3
P3(G-2)/D_2O	1340.2	536.1				1.6

[a] Molecular weight and polydispersity of PS/CS_2 are taken from ref 21.

sufficient scattering intensity. The scattered intensity was put on absolute scale by calibration with water ($I_{H_2O}^{d=1mm} = 0.857$ cm^{-1}).[7]

The scattering intensity for dilute solutions is given by

$$I(q) = kcM_wP(q)\,S(q) \tag{1}$$

where c is the concentration (in [g/mL]), M_w the weight-average molecular weight, $P(q)$ the (z-average) form factor, and $S(q)$ the intermolecular structure factor.

The neutron contrast factor k is defined as

$$k = N_L\left[\frac{\sum_i b_{2,i}}{m_2} - \frac{\rho_1}{\rho_2}\frac{\sum_i b_{1,i}}{m_1}\right]^2 \tag{2}$$

where b_i are the atomic scattering cross sections of the solvent (1) and the monomer unit (2) (in [cm]), m_i are the molecular weights of the solvent and monomer (in [g/mol]), and ρ_i are the specific densities (in [g/cm^3]) or inverse partial specific volumes $v_i = \rho_i^{-1}$ (in [cm^3/g]). The specific densities have been measured with a density meter (Paar DMA602). The measured densities of the solvents are $\rho_1 = 0.942$ g/cm^3 for perdeuterated benzene and $\rho_1 = 0.885$ g/cm^3 for perdeuterated methanol. The specific densities of the polymers are listed in Table 1. They are in the range 1.2−1.3 g/cm^3, which is typical for aromatic polyethers such as phenoxy resins (1.18−1.3 g/cm^3) or aromatic polyether amides (1.1−1.3 g/cm^3).[8] The density data in D_2O were not determined, since strong electrostatic interactions prevented reliable extrapolation to zero-angle scattering intensity $I(0)$ for the determination of molecular weights.

Form Factor of Excluded-Volume Chains

The structure of polymers is an important field of application for small-angle scattering methods. These investigations often provide information not obtainable by other methods. Polymers can have a fairly complicated conformational structure and are practically always polydisperse. Therefore, special models are used for analyzing the structure of polymers. The simplest model is the Gaussian chain. It consists of N linked segments of length l where the distance between two segments follows a Gaussian distribution. For rigid polymers the persistent (wormlike) chain model is more appropriate. This model allows to represent both rigid and flexible macromolecular chains. Within this model there is a transition from the behavior of a Gaussian chain to the behavior of a rigid rod at a certain length scale (persistence length) which serves as a measure of chain rigidity. The Gaussian and persistent chain model ignore long-range interactions in the macromolecule. These interactions are parametrized in terms of the excluded volume. It turned out that, for the polymers investigated in the present study, excluded-volume interactions dominate the conformational properties. In the following we will therefore give a more detailed description of the scattering behavior of excluded-volume chains.

The excluded-volume or self-avoiding effect of polymer chains is one of the classical problems in polymer physics. In the presence of excluded volume, the probability distribution function $P(r)$ of the distance r between two monomers deviates from the Gaussian distribution. Approximate expressions for the probability distribution function have been derived either from renormalization group (RNG) calculations or from Monte Carlo (MC) simulations. It is now commonly accepted that the distribution function suggested by des Cloiseaux[9,10] where

$$p(r) \sim r^{2+\theta}\exp[-r^\delta] \tag{3}$$

with the exponents $\delta = 1/(1-\nu)$ and $\theta = (\gamma-1)/\nu$ gives the best description of an excluded-volume chain.[11,12] The two critical exponents γ and ν are related to the chain entropy and chain size, respectively.[13] For chains of finite length, the critical exponents depend on the actual position of the chain segments on the chain contour. In the long-chain limit, their value only depends on the dimensionality d, i.e., for $d = 3$, $\gamma = {}^4/_3$, and $\nu = {}^3/_5$. From RNG theory the best estimates for $d = 3$ are currently $\nu = 0.588$ and $\gamma = 1.1619$.[14]

The form factor of an excluded-volume chain is derived from the normalized pair distribution function $P(r)$ as[15]

$$P(r) = \frac{B}{X^3}\left(\frac{r}{X}\right)^{2+\theta}\exp\left[-D\left(\frac{r}{X}\right)^\delta\right] \tag{4}$$

with $X = (R_0^2/3)^{1/2}$. The normalization constants are obtained from the conditions $\int_0^\infty P(r)4\pi r^2\,dr = 1$ and $\int_0^\infty r^2P(r)4\pi r^2\,dr = R_0^2$, yielding $D = \{(1/3)(\Gamma[(7+\theta)/\delta])/(\Gamma[(5+\theta)/\delta])\}^{\delta/2}$ and $B = (\delta/4\pi)[D^{(5+\theta)/\delta}/(\Gamma[(5+\theta)/\delta])]$ where $\Gamma[z]$ is the gamma function. The mean-square end-to-end distance is given by $R_0^2 = n^{2\nu}b^2$ with n the number of segments and b the segment length. The form factor of the excluded-volume chain is obtained from Fourier transformation of $P(r)$[16]

$$P(q) = 2\sum_{n=0}^{\infty}\frac{\Gamma[3/2]]}{\Gamma[(3+n)/2]}\frac{\Gamma[(5+\theta+2n)/\delta]}{\Gamma[(3+\theta+2n)/\delta]}\times \frac{(1+2\nu)^n\,(2+2\nu)^n}{(1+2\nu n)(2+2\nu n)}\frac{1}{n!}\left(-\frac{q^2{R_g}^2}{12D^{2/\delta}}\right)^n \tag{5}$$

In the case $\nu = {}^1/_2$, $\gamma = 0$ this expression reduces to the

Table 2. Results from the Analysis of the SANS Curves: Scattered Intensity $I(0)$, Weight-Average Molecular Weight M_w^{SANS}, Calculated Degree of Polymerization N_w, Cylinder Length L_z, Radius of Gyration $R_{g,z}$, Flory Exponent ν, Critical Exponent γ, Cross-Sectional Radius R_D, and Characteristic Scattering Vector q^*

sample	$I(0)$ (cm^{-1})	M_w^{SANS} (g/mol)	N_w	L_z (Å)	$R_{g,z}$ (Å)	ν	γ	R_D (Å)	q^* (Å^{-1})
PS/CS_2			480		93.9	0.57	−0.15	7.1	0.224
P1(G-1)/C_6D_6	1.03	124 000	275		96.4	0.58	−0.20	15.8	0.111
P1(G-2)/C_6D_6	13.6	2 210 000	2530		288	0.56	0.86	23.1	0.086
P1(G-3)/C_6D_6	4.35	401 000	233	496				25.2	
P2(G-1)/CD_3OD	5.23	437 000	650		127	0.46	0.05	19.1	0.091
P2(G-2)/CD_3OD	2.60	275 000	188	294	78.2	0.44	0.11	25.1	0.076
P3(G-1)/D_2O	0.383		650		(86.4)	0.85	−0.69	13.4	0.063
P3(G-2)/D_2O	0.467		188	211				19.1	

well-known Debye function[17]

$$P(q) = 2\sum_{n=0}^{\infty}\frac{(-x)^n}{(n+2)!} = 2\left(\frac{e^{-x}}{x^2} + \frac{1}{x} - \frac{1}{x^2}\right) \qquad (6)$$

with $x = q^2R_g^2$. The radius of gyration is related to the contour length L and the Flory exponent ν as

$$R_g^2 = \frac{b^2N^{2\nu}}{(1+2\nu)(2+2\nu)}$$
$$L = Nb \qquad (7)$$

with the two limiting cases of a Gaussian chain ($\nu = {}^1/_2$) where $R_g^2 = Nb^2/6$ and the cylinder ($\nu = 1$) where $R_g^2 = N^2b^2/12$.

At large q values, the form factor of a polymer chain is expected to reflect its locally cylindrical structure. The form factor of long cylinders ($L \gg D$) is given by[18]

$$P_{cyl}(q) = P_L(q)\,P_D(q) \qquad (8)$$

where $P_L(q)$ is the form factor of an infinitely thin cylinder

$$P_L(q) = \frac{2}{qL}\mathrm{Si}(qL) - \left(\frac{\sin(qL/2)}{qL/2}\right)^2 \qquad (9)$$

and $P_D(q)$ is the cross-sectional form factor

$$P_D(q) = \left(\frac{2J_1(qR_D)}{qR_D}\right)^2 = {}_0F_1{}^2\left(2; -\frac{q^2R_D{}^2}{4}\right) \qquad (10)$$

Si(z) is the sine integral, $J_1(z)$ the Bessel function, and ${}_0F_1(z)$ the hypergeometric function.[16] The cross-sectional form factor is averaged over a Schulz−Zimm distribution[19]

$$P_D(q) = \int_0^\infty P(q,R_D)\,h(R_D)\,dR_D$$
$$h(R_D) = \frac{(z+1)^{z+1}R_D{}^z}{\langle R_D\rangle^{z+1}\Gamma(z+1)}\exp\left[-\frac{(z+1)R_D}{\langle R_D\rangle}\right] \qquad (11)$$

with the average cross-sectional radius $\langle R_D\rangle$ and the relative standard deviation $\sigma = (z+1)^{-1/2}$. The integral can be obtained analytically when representing $P_D(q)$ as a hypergeometric function as outlined in ref 16.

Numerical approximations have been developed to interpolate between the form factor of an excluded-volume chain and a cylinder.[20] For the determination of characteristic chain parameters (L, R_g, b, ν, γ, R_D) of the dendritic PS chains, the low-q part ($q < q^*$) and high-q part ($q > q^*$) were analyzed separately (excluded-volume chain, cylinder) under the constraint of having a continuous scattering curve over the whole q range. The q value separating the low- and high-q part, q^*, is a measure of chain stiffness. The parameters are obtained from a nonlinear least-squares fit to the measured scattering curve using the Levenberg−Marquardt algorithm and are summarized in Table 2. The relative errors of the fit parameters as calculated from the covariance matrix are all between 1 and 5% except for the parameter γ, where the relative error is 10%.

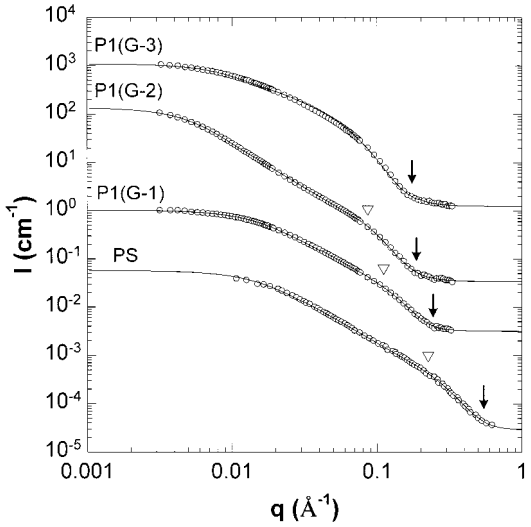

Figure 2. Measured scattering curves for P1(G-1), P1(G-2), and P1(G-3) in benzene-d_6. The data for PS in CS_2 are taken from ref 20. The scattering curves have been vertically shifted by multiplication with a factor of 5×10^{-5} (PS), 1 (P1(G-1)), 10 (P1(G-2)), and 400 (P1(G-3)) to visualize characteristic trends in the scattering behavior. The arrows indicate the position of the first minimum of oscillations in the Porod regime. The position is inversely proportional to the cross-sectional diameter $2R_D$, which increases systematically from PS to P1(G-1), P1(G-2), and P1(G-3). The triangles separate the excluded-volume behavior at low q from rodlike behavior at large q and indicate the value of q^*. Solid lines are nonlinear least-squares fits. P1(G-3) can be adequately described by a cylinder over the whole q range.

Results and Discussion

The scattering curves of PS, P1(G-1), P1(G-2), and P1-(G-3) are displayed in Figure 2. The data for PS in CS_2 have been taken from ref 21. The scattering curves are shifted vertically to visualize characteristic trends.

At intermediate scattering vectors $0.01 \le q \le 0.1$ Å^{-1} PS, P1(G-1), and P1(G-2) have a characteristic $I \sim q^{-1/\nu}$ behavior with Flory exponents $\nu \approx 0.57$ typical for polymers in good solvents. P1(G-3) exhibits the scattering behavior of a cylinder over the whole q range. The Porod q^{-4} behavior at large q corresponds to the scattering of a thick cylinder with cross-sectional radius R_D. The arrows indicate the position of the first damped

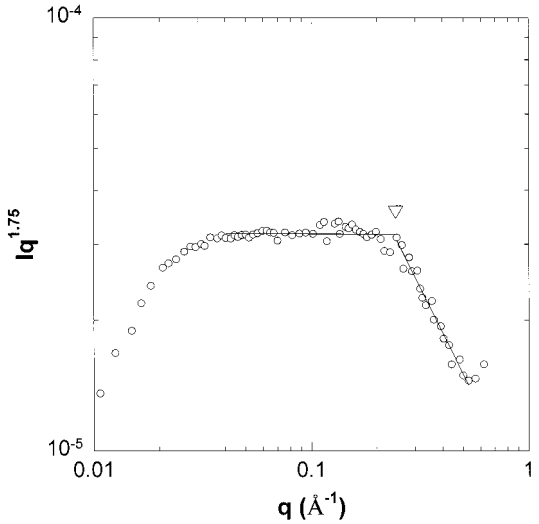

Figure 3. Kratky-type plot of the scattered intensity $Iq^{1/\nu}$ ($\nu = 0.57$) vs q for PS/CS_2. The tangential construction is used for the determination of q^*, indicated by the triangle. We note the absence of the $I(q) \approx q^{-1}$ behavior at intermediate q that would be expected for Kratky−Porod-type chains.

oscillation which systematically shifts from $q_D \approx 0.55$ Å^{-1} for PS corresponding to $R_D = 7.1$ Å to $q_D \approx 0.15$ Å^{-1} corresponding to $R_D = 25.2$ Å for P1(G-3).

The solid lines are fits to the excluded-volume form factor (eq 5) at low q and the form factor of a cylinder (eq 8) at high q. The scattering vectors q^* dividing the two fit regimes are indicated by triangles. The fits yield the scattered intensity $I(0)$, the radius of gyration R_g, the Flory exponent ν, the critical exponent γ, and the cross-sectional radius R_D. The values are summarized in Table 2. P1(G-3) is best described over the whole q range by the form factor of a cylinder. The fitted cylinder length is also given in Table 2. From the scattered intensity $I(0)$, the molecular weight M_w together with the degree of polymerization N_w is determined using eq 1.

It is interesting to note that the scattering curves cannot be described by a Kratky−Porod chain that exhibits as characteristic features a $I(q) \sim q^{-2}$ behavior at intermediate q with a crossover to a $I(q) \sim q^{-1}$ behavior at large q. Instead, the scattering curves exhibit excluded-volume behavior $I(q) \sim q^{-1/\nu}$ ($\nu \approx 0.57$ in good solvent, $\nu \approx 0.45$ in bad solvent) at intermediate scattering vectors until it enters the Porod q^{-4} behavior at large q. This is shown in Figure 3 in a Kratky-type plot of $Iq^{1/\nu}$ vs q for PS/CS_2. The same behavior is observed for P1(G-1), P1(G-2), P2(G-1), P2(G-2), and P3-(G-1). The tangential construction in Figure 3 is used for the determination of q^*.

Often, the Kratky−Porod chain model is used to determine Kuhn lengths from measured contour lengths and radii of gyration. For Kratky−Porod chains the radius of gyration is given by

$$R_g^2 = \frac{Lb}{6} - \frac{b^2}{4} + \frac{b^3}{4L} - \frac{b^4}{8L^2}\left(1 - \exp\left[-\frac{2L}{b}\right]\right) \quad (12)$$

As discussed above, the Kratky−Porod model does not adequately describe the structure of the polymer chains in the present investigation. We include these values for comparison with results published in the literature.[4,22]

To obtain the statistical segment length or Kuhn length b_w from eq 7 (or eq 12), the measured z-average radius of gyration $R_{g,z}$ is converted to the weight-average $R_{g,w}$ via

$$\frac{R_{g,w}}{k+1} = \frac{R_{g,z}}{k+2} \quad (13)$$

with $1/k = M_w/M_n - 1$ assuming a Schulz−Zimm distribution. From the degree of polymerization N_w the weight-average contour length $L_w = N_w l_0$ can be calculated, where l_0 is the contour length of a monomer unit, i.e., the length of a monomer projected onto the contour of the polymeric backbone. For flexible vinylic polymers, l_0 is calculated from the carbon−carbon bond length $l_{cc} = 1.532$ Å assuming a tetrahedral bond angle to be $l_0 = 2l_{cc}\sqrt{2}/\sqrt{3} \approx 2.50$ Å.

From the excluded-volume chain model (eq 7), the calculated value for PS is $b_w = 22$ Å, which is in good agreement with the value of 23 Å given by Rawiso et al.[21] and may be compared to the value of 25 Å for the infinite chain limit following from the characteristic ratio of polystyrene $C_\infty = 10.0$.[23] It is expected that dendronization leads to a considerable increase of the Kuhn length. As apparent from Table 3, the values are larger compared to that of polystyrene, in the range 25−50 Å. Still, the Kuhn lengths calculated from eq 7 (or eq 12) are surprisingly small. The reason for this becomes obvious when comparing the calculated contour length of P1(G-3), $L_{w,c}$, with the measured cylinder length, L_w. We observe that L_w is only about 50% of the calculated value assuming a monomer contour length of $l_0 = 2.50$ Å. The same observation can be made for P2(G-2). It appears that the bulky side groups force the polymer backbone out of an all-trans conformation, resulting in a smaller monomer contour length.

A reduction of the chain contour can result from the formation of helices. In the crystalline state, most vinylic polymers such as isotactic polystyrene (it-PS) form a helix with three units per turn (3_1-helix). In case of it-PS, the measured helix repeat distance is $d_h = 6.5$ Å, yielding a projected contour length of $l_0 = 6.5/3 \approx 2.16$ Å. This corresponds to a reduction of the contour length to 86% of its fully extended all-trans value. Vinyl polymers with bulkier side groups such as it-poly(*o*-methylstyrene) or poly(vinylnaphthalene) form 4_1-helices.[24] The dendronized polystyrenes may similarly form helices in solution, leading to a considerable reduction of the chain contour.

To estimate the reduction of the contour length in case of the flexible dendronized polymers, we determine the Kuhn lengths directly from the scattering curves. As discussed above, the measured value of q^* sets a length scale $d^* = 2\pi/q^*$, below which the polymer chain can be described as a cylinder. This corresponds to the original idea of a Kuhn length or a statistical segment length. We may convert the characteristic length d^* to the corresponding Kuhn length b^* by multiplying it with the ratio $c = b_{PS}/d_{PS}^* = 0.79$ obtained for polystyrene. Within this operational definition of the Kuhn length b^*, polystyrene serves as a reference for a polymer chain with a monomer contour length following from an all-trans conformation which is describable in terms of the excluded-volume chain model. Values of b^* are summarized in Table 3. b^* is increasing from 22 Å for PS to 53 Å for P1(G-1) and 56 Å for P1(G-2). For P1(G-3) the statistical segment length is of the order of the contour

Table 3. Calculated Cylinder Length L_w (Eq 13), Radius of Gyration $R_{g,w}$ (Eq 13), Hypothetical Contour Length Assuming All-Trans Conformation $L_{w,c}$, Calculated Kuhn Lengths b_w (Eq 7) and b_w^{KP} (Eq 12), Rescaled Kuhn Length b^*, Ratio of Kuhn Length and Cross-Sectional Radius b^*/R_D, Rescaled Contour Length L^*, and Contraction Factor of the Chain Contour $L^*/L_{w,c} = l^*/l_0$

sample	L_w (Å)	$R_{g,w}$ (Å)	$L_{w,c}$ (Å)	b_w (Å)	b_w^{KP} (Å)	b^* (Å)	b^*/R_D	L^* (Å)	$L^*/L_{w,c}$, l^*/l_0
PS/CS_2		83.1	1200	22.1	36.1	22.1	3.1	1200	1.0
P1(G-1)/C_6D_6		70.1	688	29.5	47.5	44.7	2.8	509	0.7
P1(G-2)/C_6D_6		216	6320	25.2	44.8	57.7	2.5	3290	0.5
P1(G-3)/C_6D_6	294		583					294	0.5
P2(G-1)/CD_3OD		81.3	1630	31.3	25.0	54.5	2.9	847	0.5
P2(G-2)/CD_3OD	214	56.9	470	48.9	48.0	65.3	2.6	326	0.5
P3(G-1)/D_2O		(55.2)	1630			78.7	5.9		
P3(G-2)/D_2O	153		470						

length (294 Å). These values may be compared to that of DNA, which has a statistical segment length of 60 Å for high salt concentrations, approaching 100 Å at low ionic strength due to charge repulsion along the chain.[25]

Within the excluded-volume model we can calculate the contour length by employing the measured radius of gyration $R_{g,w}$ and Flory exponent ν to calculate the contour length L^* from eq 7. As seen from Table 3, values of L^* or l_0^* are within a range of 55−75% of the calculated all-trans contour length $L_{w,c}$ or l_0, approaching the value of 50% obtained for P1(G-3) from a direct measurement of the contour or cylinder length without relying on the definition of a Kuhn length. We observe that P1(G-1) has a reduction of chain contour length within a range typical for 3_1- or 4_1-helices. The configuration of the chain backbone in the case of a 50% contour length reduction is currently unclear.

A pecularity of P1(G-2) is the large value of the critical exponent $\gamma = 0.86$, which is close to the theoretical value of $\gamma = 1.1619$.[14] P1(G-2) has a high molecular weight which leads to nearly full development of excluded-volume effects. A large value of ν is related to the enhancement of chain configurations with widely separated chain ends. It leads to the development of a characteristic shoulder in the scattering curve, in the case of P1(G-2) in the range $0.005 \le q \le 0.01$ Å^{-1}.

P2(G-1) and P2(G-2) are examples of polymers carrying dendrons with functional groups. Figure 4 shows the measured scattering curves. The analysis yields small values of the Flory exponent $\nu \approx 0.45$, indicating that methanol is a bad solvent for these polymers. Due to the bulky functional groups the cross-sectional radius of P2(G-1) and P2(G-2) are almost as large as those of the corresponding P1(G-2) and P1(G-3) chains investigated above. The scattering curve of P2(G-2) can almost be described by a cylinder as indicated by the dotted line in Figure 4, which is a fit to eq 8.

Hydrolysis of P2(G-*x*) polymers with perfluoroacetic acid yields polyelectrolytes with 2 (for P3(G-1)) or 4 charges (for P3(G-2)) per repeat unit. The mutual repulsion of these charges leads to additional stiffening of the polymer chain. We observe a significant influence of the structure factor $S(q)$ on the scattering curve. The position $\hat{q}$ of the maximum in the scattered intensity, as apparent in Figure 5, can be related to the average distance of the polymer chains via the Bragg relation $\hat{d} = 2\pi/\hat{q}$. From the position of the maximum, we calculate an average distance of $\hat{d} = 419$ Å for P3(G-1) and $\hat{d} = 349$ Å for P3(G-2). This may be compared to the average distance calculated from the polymer concentration via

$$\hat{d}_c = \left(\frac{6}{\pi}\phi_{max}\frac{M_w}{cN_L}\right)^{1/3} \qquad (14)$$

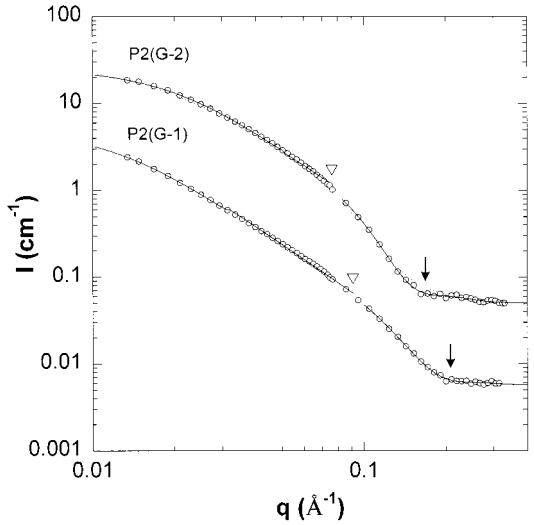

Figure 4. Measured scattering curves for P2(G-1) and P2(G-2) in methanol-d_4. The scattering curve for P2(G-2) has been shifted vertically by multiplication with a factor of 10. Arrows indicate the position of the first minimum in the Porod regime. The related cross-sectional diameter is larger for the P2(G-2) sample. The triangles indicate the value of q^*. The solid lines are nonlinear least-squares fits. P2(G-2) almost has a cylindrical conformation as shown by the comparison to the scattering curve of a cylinder (dotted line).

where ϕ_{max} is the volume fraction of maximum packing which is $\phi_{max} = 0.63$ for random close packing (rcp) assuming a fluidlike arrangement of the polymers in solution. From the volume fraction we estimate $\hat{d}_c = 419$ Å for P3(G-1) and $\hat{d}_c = 329$ Å in the case of P3(G-2), in good agreement with the measured values of $\hat{d}$.

The scattering curves of the charged dendronized polymers P3(G-1) and P3(G-2) can be well parametrized when assuming a simple form of the structure factor derived for hard spheres. Hard-sphere systems may be used to describe solutions of cylindrical or extended polymer chains if the concentration is below the overlap concentration c^* and if the electrostatic interactions are weak. Using the Percus−Yevick expression for the hard-sphere structure factor $S(q)$,[26,27] the scattering curves can be analyzed using eqs 1, 5, and 8, yielding in addition to the characteristic chain parameters L, R_g, ν, γ, and R_D the effective hard-sphere radius R_{eff} and the effective volume fraction ϕ_{eff}. Values are $R_{eff} = 1.41$ Å and $\phi_{eff} = 0.11$ for P3(G-1) and $R_{eff} = 144$ Å and $\phi_{eff} = 0.11$ for P3(G-2). The values of the corresponding effective diameters and effective volume fractions seem quite large, indicating strong interactions. They should, however, be considered with caution as the Percus−Yevick approximation assumes a simple hard-sphere system where the form of the interaction potential is steeper compared to the case of charged systems and

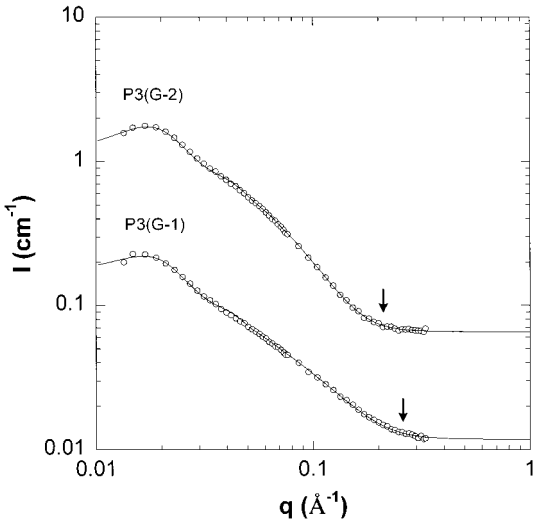

Figure 5. Measured scattering curves for charged P3(G-1) and P3(G-2) in D_2O. The scattering curve for P3(G-2) has been shifted vertically by multiplication with a factor of 5. The solid lines are nonlinear least-squares fits using the Percus−Yevick approximation for the intermolecular structure factor. The arrows indicate the position of the first minimum of oscillations in the Porod regime. The triangle indicates the value of q^*. P3(G-2) has a cylindrical conformation over the whole q range. The peaks at low q correspond to the average distance between polymer chains.

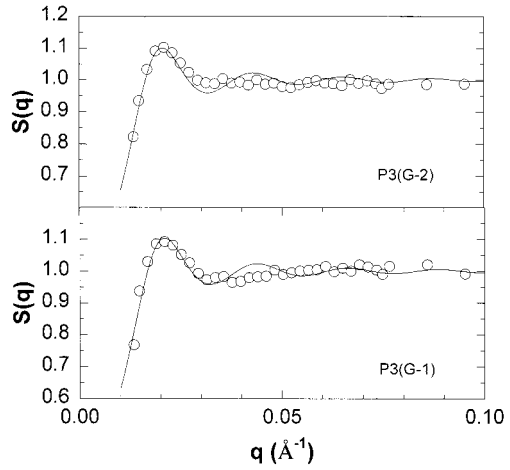

Figure 6. Measured structure factor of P3(G-1) and P3(G-2) and comparison to the Percus−Yevick approximation (solid lines). There is a noticeable decrease of $S(q)$ at low q, indicating strong repulsive interactions between the charged dendronized polymers. The peak reflects positional correlations between neighboring polyelectrolyte chains.

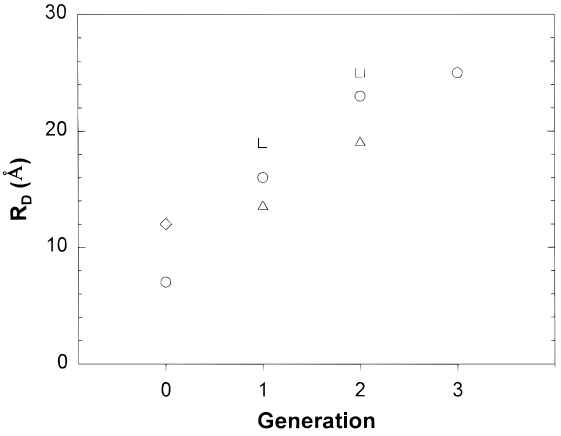

Figure 7. Measured cross-sectional radii R_D for the P1(G-x) (○), P2(G-x) (□), and P3(G-x) series (△). One notes a systematic increase of R_D with increasing generation in each series. The cross-sectional radius of DNA (◇) is included for comparison. For PS-G3 the radius seems to approach a saturation limit due to steric overcrowding. The concomitant strong increase of the bending rigidity leads to an extended rodlike conformation of the polymer chain.

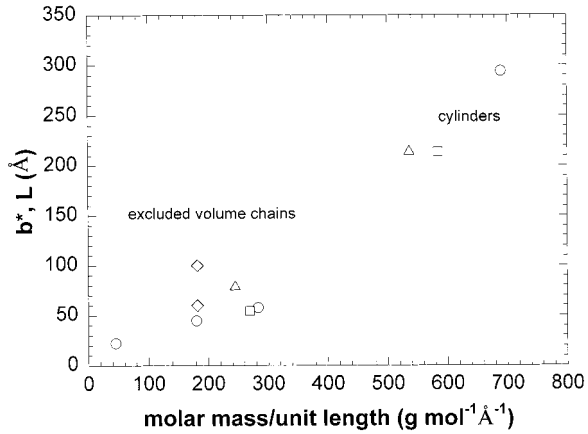

Figure 8. Measured Kuhn lengths b^* and contour lengths L_w of neutral (open symbols) and charged polymers (gray symbols) in the P1(G-x) (○), P2(G-x) (□), and P3(G-x) series (▲) as a function of mass per unit length. Polymers having an excluded-volume chain conformation (PS, P1(G-1), P1(G-2), P2-(G-1), P3(G-1)) are characterized by their Kuhn lengths, while polymers with a cylindrical structure (P1(G-3), P2(G-2), P2-(G-3)) are characterized by their cylinder length. The range of values for DNA at different salt concentrations is included for comparison (◆). The increase of b^* is approximately proportional to the increase in cross-sectional diameter D ($b \approx 1.4D$). For P1(G-3) and, to a lesser extent, for P2(G-2) steric overcrowding leads to further strong increase of b^*.

therefore may not give true effective radii and volume fractions. Nevertheless, the Percus−Yevick structure factor allows a simple parametrization of the scattering curve to capture the main features of $S(q)$. Figure 6 displays the structure factor for P3(G-1) and P3(G-2). Both exhibit a peak at $q \approx 0.02$ Å^{-1} and a pronounced decrease at low q, typical for a liquidlike structure.

The main results of this study are summarized in Figures 7 and 8. Figure 7 shows the increase of the measured chain diameter with increasing dendron generation. There is a systematic increase within the P1(G-x), P2(G-x), and P3(G-x) series. P2(G-2) with its bulky substituents exhibits almost the same diameter as P1(G-3). Interestingly, the measured diameters for the charged P3(G-x) series are significantly smaller compared to those of the P2(G-x) series due to shorter functional groups, but possibly also because the hydrophobic dendron moieties collapse onto the chain backbone in aqueous medium. The diameters of the dendronized polymer chains can be compared to those of DNA with a value of $d = 24$ Å.[25]

The attachment of bulky dendrons to a polystyrene backbone is expected to lead to an increase of the statistical segment length. In Figure 8 the measured Kuhn lengths are plotted as a function of mass per unit length (g/mol Å) to compare different types of dendrons (P1(G-x), P2(G-x), and P3(G-x) series, DNA). As a rule of thumb, the segment length $b^* \approx 2.8R_D$ for uncharged, flexible excluded-volume chains (Table 3). As the persistence length a is half the Kuhn length and equal to the local curvature radius R_c of the chain contour, we have $R_c \approx 1.4R_D$. It appears that the cross-sectional

radius R_D sets a basic length scale for the curvature radius R_c. The ratio of R_c and R_D is determined by the local curvature energy which points to an interesting analogy to toroidal vesicle structures. Similar to the local structure of a polymer chain, a toroid is defined by its cross-sectional radius R_D and the radius of its rim R_c. In case of vesicles the Clifford torus with a ratio $R_c = \sqrt{2}R_D$ minimizes the curvature energy with a similar ratio of R_c and R_D.[28]

Charged polymers exhibit a significant further increase of b^*. For polymers with bulky high-generation dendrons (P3(G-2), P1(G-3)) steric overcrowding with the concomitant increase in bending rigidity leads to an extended cylindrical structure. For these polymers the cylinder length L is the appropriate measure for the chain conformation and is therefore included for comparison in Figure 8. The values can be compared to those of DNA, a well-investigated example of a semiflexible polymer chain. With an average of 618 g/mol (two base pairs) per 3.4Å (distance between two base pairs in the double helix), we calculate a mass of 182 g/(mol Å). Measured Kuhn lengths are in the range $60 \leq b \leq 100$ Å, which are well in the range observed with dendronized polymer chains, considering that the larger values are due to charge repulsion along the DNA double helix at low ionic strength.

Conclusions

The dendronization of polymer chains is a unique way to induce chain stiffness in a well-defined manner. The changes in chain conformation can be followed by small-angle neutron scattering. The scattering curves can be analyzed quantitatively with form factors of excluded-volume chains and cylinders to obtain the contour length, radius of gyration, the statistical segment length, the critical exponents of excluded-volume chains (ν and γ), and the chain diameter. For flexible, uncharged chains the segment length is proportional to the chain diameter. High molecular weight P1(G-2) exhibits a pronounced enhancement of chain conformation with widely separated chain ends, an expected effect for long excluded-volume chains. Polymer chains with high-generation bulky substituents have a cylindrical conformation due to steric overcrowding and the concomitant increase in bending rigidity. These factors force the chain backbone out of its all-trans conformation, leading to smaller chain contour lengths. The introduction of charges on the dendrons leads to further chain expansion in aqueous solution and positional ordering as reflected in the structure factor.

Acknowledgment. Financial support of the Dr.-Hermann-Schnell Foundation, the Fonds der Chemischen Industrie (FChI), and the German Science Foundation (SFB 448, TPA1) is gratefully acknowledged. We also thank M. Schmidt for valuable comments.

References and Notes

(1) Newkome, G. R.; Moorefield, C. N.; Vögtle, F. *Dendritic Molecules—Concepts, Syntheses, Perspectives*; VCH: Weinheim, 1996.
(2) Schlüter, A. D. In *Topics in Current Chemistry;* Vögtle, F., Ed.; Springer: Berlin, 1998; Vol. 197; p 165.
(3) Stocker, W.; Schürmann, B. L.; Rabe, J. P.; Förster, S.; Lindner, P.; Neubert, I.; Schlüter, A. D. *Adv. Mater.* **1988**, *10*, 793.
(4) Neubert, I.; Amoulong-Kirstein, E.; Schlüter, A. D.; Dautzenberg, H. *Macromol. Rapid Commun.* **1996**, *17*, 517.
(5) Neubert, I.; Schlüter, A. D. *Macromolecules* **1998**, *31*, 9372.
(6) The molecular weights obtained from GPC correspond to the molecular weights of equivalent polystyrene chains having the same elution volume.
(7) Lindner, P. In *Modern Aspects of Small-Angle Scattering*; Brumberger, H., Ed.; NATO Advanced Study Institutes, Series C; Kluwer Academic: London, 1993; Vol. 451.
(8) Brydson, J. A. *Plastics Materials*, 6th ed.; Butterworth & Heinemann: Oxford, 1995.
(9) des Cloiseaux, J. *Phys. Rev. A* **1974**, *10*, 1665.
(10) des Cloiseaux, J. *J. Phys. (Paris)* **1985**, *41*, 223.
(11) Bishop, M.; Clarke, J. H. R. *J. Chem. Phys.* **1991**, *94*, 3936.
(12) Valleau, J. P. *J. Chem. Phys.* **1996**, *104*, 3071.
(13) de Gennes, P.-G. *Scaling Concepts in Polymer Physics*; Cornell University Press: Ithaca, NY, 1979.
(14) Macdonald, D.; Hunter, D. L.; Kelly, K.; Jan, N. *J. Phys. A* **1992**, *25*, 1429.
(15) Wittkop, M.; Kreitmeier, S.; Göritz, D. *J. Chem. Phys.* **1996**, *104*, 351.
(16) Förster, S.; Burger, C. *Macromolecules* **1998**, *31*, 879.
(17) Debye, P. *J. Phys. Colloid Chem.* **1947**, *51*, 18.
(18) Neugebauer, T. *Ann. Phys.* **1943**, *4*, 35.
(19) Schulz, G. V. *Z. Phys. Chem. (Munich)* **1939**, *43*, 25.
(20) Pedersen, J. S.; Schurtenberger, P. *Macromolecules* **1996**, *29*, 7602.
(21) Rawiso, M.; Duplessix, R.; Picot, C. *Macromolecules* **1987**, *20*, 630.
(22) Percec, V.; Ahn, C.-H.; Cho, W.-D.; Jamieson, A. M.; Kim, J.; Leman, T.; Schmidt, M.; Gerle, M.; Möller, M.; Prokhorova, S. A.; Sheiko, S. S.; Cheng, S. Z. D.; Zhang, A.; Ungar, G.; Yeardley, D. J. P. *J. Am. Chem. Soc.* **1998**, *120*, 8619.
(23) Brandrup, J.; Immergut, E. H. *Polymer Handbook*; Wiley & Sons: New York, 1989.
(24) Gaylord, N. G.; Mark, H. F. *Linear and Stereoregular Addition Polymers;* Interscience: New York, 1959.
(25) Kassapidou, K.; Heenan, R. K.; Jesse, W.; Kuil, M. E.; van der Maarel, J. R. C. *Macromolecules* **1995**, *28*, 8, 3230.
(26) Percus, J. K.; Yevick, G. J. *Phys. Rev.* **1958**, *110*, 1.
(27) Ashcroft, N. W.; Lekner, J. *Phys. Rev.* **1966**, *45*, 33.
(28) Jülicher, F.; Seifert, U.; Lipowsky, R. *J. Phys. II (Paris)* **1993**, *3*, 1681.

MA9817929